IEEE Access
Multidisciplinary | Rapid Review | Open Access Journal

Received February 19, 2021, accepted March 12, 2021, date of publication March 19, 2021, date of current version March 30, 2021.

Digital Object Identifier 10.1109/ACCESS.2021.3067340

An Electrically Small Frequency Selective Loop Antenna for Shielding Effectiveness Measurement

KI BAEK KIM[1], DAE HEON LEE[1], SEUNG KAB RYU[1], AND HOSUNG CHOO[2], (Senior Member, IEEE)

[1]Affiliated Institute of Electronics and Telecommunications Research Institute, Daejeon 34044, South Korea
[2]School of Electronic and Electrical Engineering, Hongik University, Seoul 04066, South Korea

Corresponding author: Hosung Choo (hschoo@hongik.ac.kr)

ABSTRACT This paper proposes an electrically small and frequency selective loop (FSL) antenna for shielding effectiveness (SE) measurement in low frequency (10 kHz – 30 MHz) magnetic fields. The proposed antenna consists of an outer loop and an inner loop. A low-pass filter is placed between outer and inner loop to improve the antenna factor (AF) in the upper frequency band as the number of loop turns increases. The size of the designed antenna is 220 mm × 220 mm, which achieves 46 % reduction of the antenna area compared to conventional 300 mm loop antennas and the proposed antenna preserves the AF characteristic over the entire frequency range (10 kHz – 30 MHz). In addition, the loop of the designed antenna is printed using microstrip techniques, which reduces the cost and complexity of the antenna fabrication. The results demonstrate that the proposed antenna is suitable for SE measurements of small enclosures (all dimensions between 0.75 m and 2 m).

INDEX TERMS Electrically small loop antenna, frequency selective antenna, SE measurement small enclosures.

I. INTRODUCTION

In the fields of high power electro-magnetic (HPEM) and electromagnetic compatibility (EMC), it is important to accurately evaluate the performance of a shielding effectiveness (SE). In particular, it is difficult to measure the SE of small enclosures with all dimensions from 0.75 m to 2 m in the low frequency (10 kHz to 30 MHz) band. The SE measurement of small enclosures in low frequency band cannot be conducted according to the actual standards in [1] and [2], since the required loop antennas [3] are too large for the small-size enclosures under test [4].

Several loop antennas for SE measurement have been developed [5]–[12]. Moebious loop structures [5]–[7], loop with a parasitic element [8], [9], and a shielded conducting surface structures [10]–[12] are reported. However, these antennas are not applicable to the small enclosures due to large volume.

In [13] and [14], 1-turn small shielded loop antenna for SE measurement is used, but the small diameter (50 mm to 60 mm) has a disadvantage of having a high antenna factor (AF) values (53.4 dB @ 10 kHz). In [15], a loop antenna with an inverted-L matching circuit is proposed, but the frequency bandwidth is narrow. In [16], the spherical dipole antenna is not suitable for magnetic field SE measurements, and loops in [17]–[19] are also too large for small enclosures. In addition, the antenna efficiency decrease by the near-ground effect of the enclosure [15].

To overcome the size problem of loop antennas, various miniaturization techniques of loop antennas have been studied, such as employing printed structure [20], adding lumped elements [21], using ceramic material [22] and using multi-turn loop [23]. These techniques can reduce the physical size of loop antennas, but have limitations in complex fabrication and reduced radiation efficiency.

The ohmic resistance of small loops is in general much larger than the radiation resistance, and thus radiation efficiencies and antenna gain are low and greatly dependent on the ohmic resistance [18]. In an effort to increase the radiation efficiency and reduce the size of the loop, multi-turn structures or ferrite cores are typically employed.

Increasing the number of loop turns improves antenna factor (AF) characteristics in the lower frequency band, but the antenna inductance increases in the upper frequency band,

The associate editor coordinating the review of this manuscript and approving it for publication was Abhishek K. Jha.

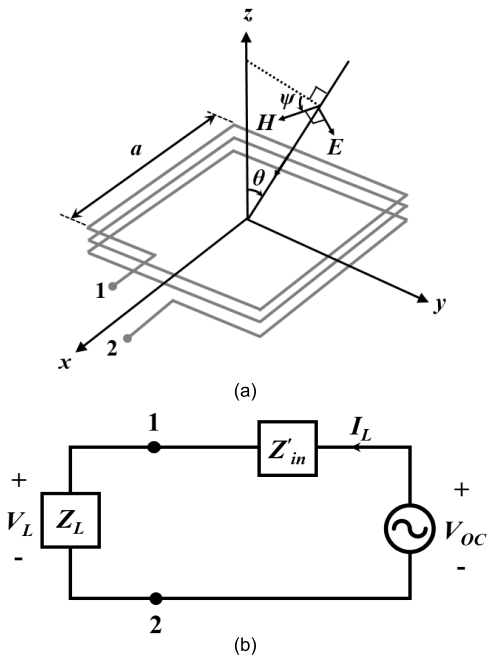

FIGURE 1. The conceptual figure of rectangular multi-turn loop antenna. (a) Plane wave incident on a receiving loop. (b) Thevnin equivalent circuit model.

which results in worse AF characteristics than a single-turn loop [24]. The ferrite core can improve the radiation efficiency, but has limitations in reducing the size of loop antenna [25]–[27].

In this paper, a novel design of a compact frequency selective loop (FSL) antenna is presented. The designed antenna has a rectangular spiral structure (1-turn outer loop, 2-turns inner loop). A low-pass filter (a parallel capacitor) is placed between the outer and the inner loops to improve the AF characteristic by reducing the inductance of the loop in the upper frequency band. Therefore, the proposed antenna is suitable for SE measurements of small-sized enclosures, where the standard such as IEEE Std. 299.1 are not applicable. Numerical and experimental results of this antenna will be presented and discussed in the following sections.

II. ANTENNA DESIGN

A. MULTI-TURN LOOP ANTENNA CHARACTERISTICS

Fig. 1(a) presents a geometry of the rectangular multi-turn loop antenna in a receiving mode with a side length a and N turns. The center of the multi-turn loop antenna is located at the origin, and the incident electromagnetic waves toward the antenna have a tilted angle ψ in the plane of incidence and θ along the z-axis. The receiving loop antenna can be described by a Thevenin equivalent circuit [28] as shown in Fig. 1(b). The open circuit voltage (V_{OC}), as written in (1), is induced between the output terminals 1 and 2.

$$V_{OC} = j\omega a^2 \mu_0 H \sin\theta \cos\psi N \tag{1}$$

where ω is the angular velocity of the wave, μ_0 is the permeability in free space, and H is the magnetic field intensity. The load voltage V_L can be calculated by the voltage ratio of the input and load impedances as expressed in (2). Then, the AF of the loop antenna is derived from the

ratio between the magnetic field intensity and the load voltage as noted in (3).

$$V_L = V_{OC} \frac{Z_L}{Z'_{in} + Z_L} = I_L Z_L \tag{2}$$

$$\begin{aligned} \mathrm{AF}_{(\mathrm{magnetic})} &= 20\log_{10}\left(\frac{H}{I_L}\right) \\ &= 20\log_{10}\left(\frac{9.73}{\lambda\sqrt{G(\mathrm{num})}}\right) - 51.5 \end{aligned} \tag{3}$$

where λ is the wavelength, G is the antenna gain.

The radiation resistance and efficiency of the small loop can be further increased by winding multi-turn loops or adding a ferrite core with high permeability. The radiation resistance (R_r) of the small loop becomes [24]

$$R_r \approx 320\pi^4 \mu^2 N^2 \left(\frac{A}{\lambda^2}\right)^2 \tag{4}$$

where μ is the effective relative permeability of the ferrite core, N is the number of loop turns, A is loop's area, and λ is wavelength. The compact size of the loop antenna is to decrease the radiation resistance (R_r) because the area (A) of the loop antenna is also reduced.

In order to compensate for this, it is necessary to increase the N. The reactance and magnetic AF with different N are simulated and shown in Fig. 2. The FR-4 is used as the substrate, and its dimensions are 220 mm × 220 mm. The width and the gap of the line are 1.5 mm and 2 mm in Fig. 2(a), respectively. In Fig. 2(b), the inductance of the loop rises rapidly above 1 MHz as N increases. In Fig. 2(c), as a reference, the AF of a commercial loop antenna [3] with diameter of 300 mm is shown (dashed line). As N increases, the AF is improved below 1 MHz, while the AF level above 1 MHz increases. As described before, this is caused by the increased inductance of the loop.

B. FREQUENCY SELECTIVE LOOP ANTENNA DESIGN

To maintain the AF improvement effect in lower frequency band (below 1 MHz) and compensate for the AF performance degradation in the upper frequency band (above 1 MHz) as the N increases, we propose the frequency selective loop antenna as shown in Fig. 3. The size of the proposed antenna is 220 mm × 220 mm and it has printed structure using the FR-4 ($\varepsilon_r = 4.6$, thickness = 1.6 mm) substrate. The designed antenna in Fig. 3(a) consists of one turn outer loop and two turns inner loop. The outer and inner loops are apart by G to minimize the coupling between loops. The low-pass filter (a parallel chip capacitor) is located between the outer and inner loop. A parallel chip resistor is connected with the inner loop on the bottom side in Fig. 3(b). A detailed view of the feeding part is shown in Fig. 3(c). Vias with a diameter of 1 mm are used to connect front and rear lines of the antenna.

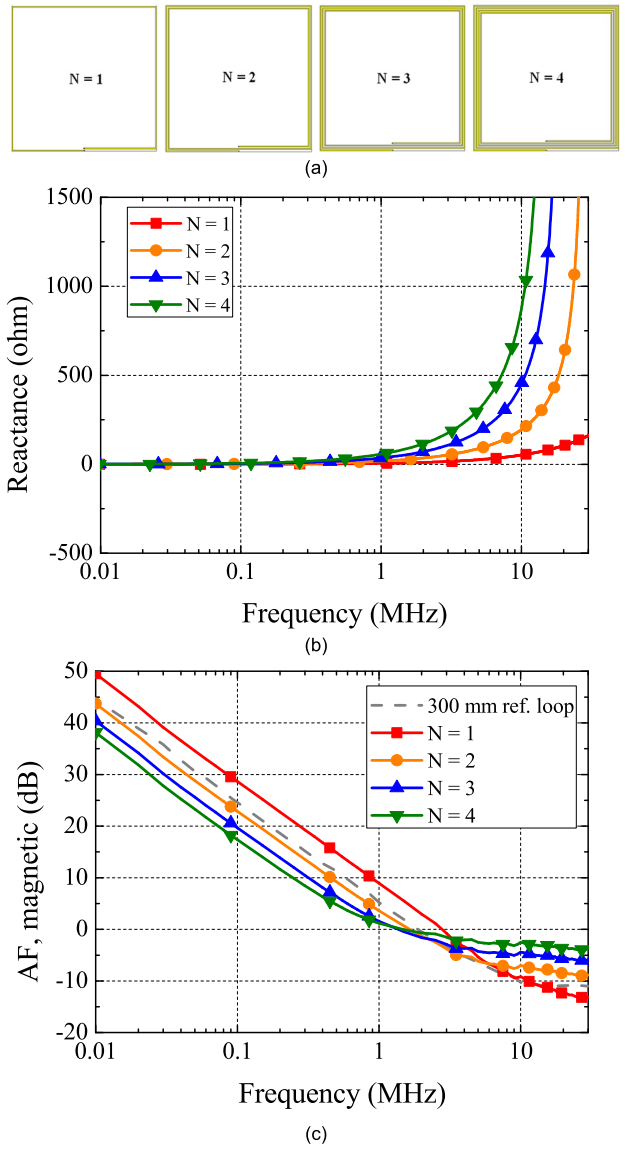

FIGURE 2. Multi-turn loop antenna characteristic with different N. (a) Structures of the multi-turn loop. (b) Reactance of the multi-turn loop. (c) AF of the multi-turn loop.

Fig. 4 shows the equivalent circuit of the proposed antenna. The parallel capacitor (1st order low-pass filter) is located between the outer loop and the inner loop.

In the lower band, the current passes through both the outer and inner loops, so the AF characteristic is improved due to the multi-turn loop. A resistor connected in parallel with the inner loop has a higher resistance value than the inner loop line and does not operate in the lower band (the current does not pass through the resistor).

In upper band, due to the low-pass filter, only outer loop operates as the antenna. The coupled current with the outer loop flows in the inner loop where the current is cut off. Thereafter the coupled current of the inner loop is attenuated by the parallel resistor.

If the value of the distance G (between the outer and inner loop) increases, the coupling current decreases at upper band.

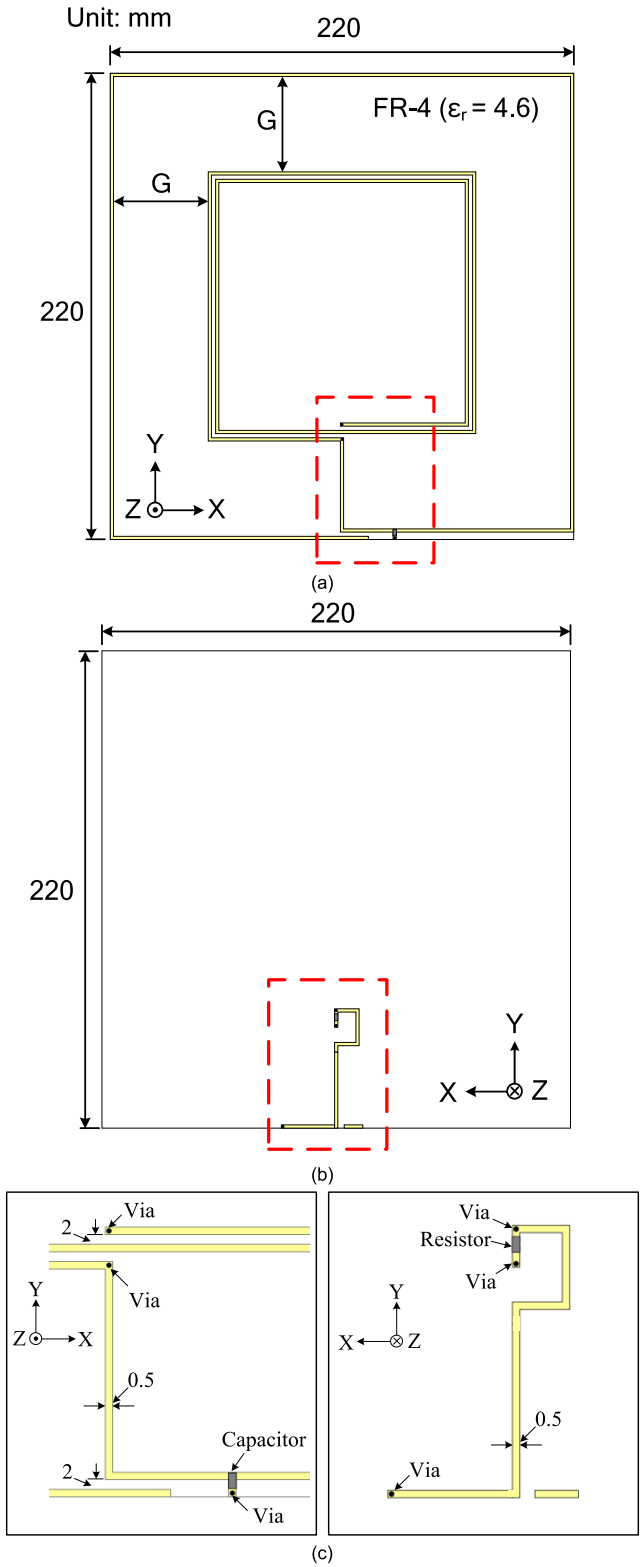

FIGURE 3. Configuration of the designed antenna. (a) Top view. (b) Bottom view. (c) Detail view of feeding part.

Therefore, G is optimized to 45 mm considering the AF since the total length of the inner loop decreases. To further improve the AF characteristic, the circuit element values of

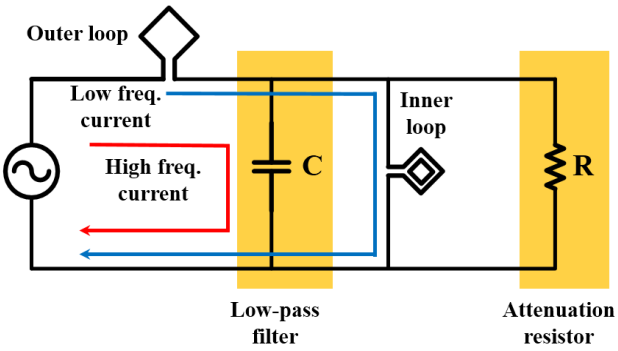

FIGURE 4. The equivalent circuit of the proposed antenna.

the proposed antenna are optimized using the full-wave EM simulation software of Microwave Studio (MWS) [29]. The optimal antenna geometric parameters are summarized in Table 1.

TABLE 1. The optimal geometric parameters of the designed antenna.

Parameters	Symbol	Value
Between the outer and inner loops	G	45 mm
Capacitance of the low-pass filter	C	820 pF
Resistance of the attenuation resistor	R	24 Ω

The mutual inductance between outer and inner loops is small enough to be ignored in the lower band with the same current direction. In upper band, the operation of the low-pass filter cuts off the current on inner loop, and the induced voltage causes a current to flow in the inner loop.

The mutual inductance between outer and inner loop can be obtained as shown in (5).

$$L_m = L_I + L_O - L_{FSL} \tag{5}$$

where L_m is the mutual inductance between outer loop and inner loop, L_I is inductance of the inner loop, L_O is inductance of outer loop, and L_{FSL} is inductance of frequency selective loop without low-pass filter (a parallel capacitor).

Fig. 5 shows the simulated mutual inductance. The mutual inductance increases from the 1 MHz where the inner loop is blocked by the operation of the low-pass filter. The maximum value of mutual inductance is 1.9 uH in operating frequency bands.

III. SIMULATED AND MEASURED RESULTS

The photograph of the fabricated antenna is shown in Fig. 6. Input port has a 50 Ω SMA connector for feeding. Fig. 7 shows the test setup for the AF measurement and simulation of the proposed antenna. In this paper, we measure the AF using the S_{21} method [30]. The transmit loop (A. H. Systems, SAS-564, 1 kHz – 30 MHz) and fabricated antenna are connected to vector network analyzer (KEYSIGHT, N5222B, 900 Hz – 26.5 GHz) port 1 and port 2, respectively. And then, the AF is calculated from the measured S_{21}.

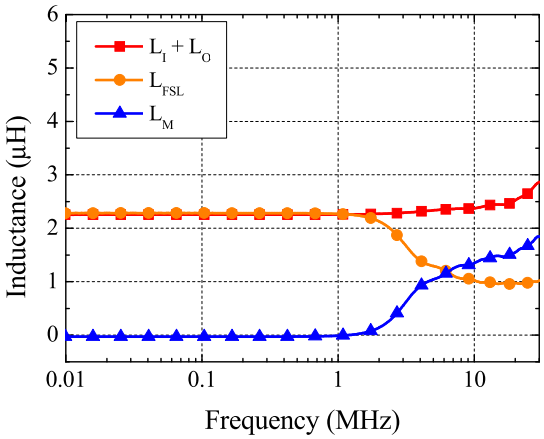

FIGURE 5. Mutual inductance of the designed antenna.

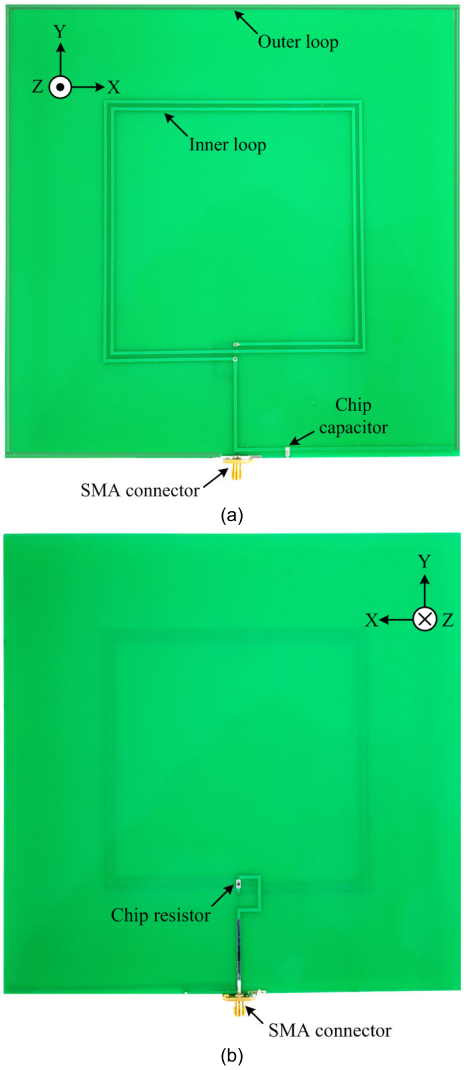

FIGURE 6. The fabricated antenna. (a) Top view. (b) Bottom view.

Fig. 8 shows a comparison of the theoretical AF ($N = 3$) in (3), the frequency selective loop (Outer $N = 3$, Inner $N = 2$) AF, and the 3-turns planer loop AF in Fig. 2(c). The total line length is FSL (3,459 mm), theory (2,638 mm),

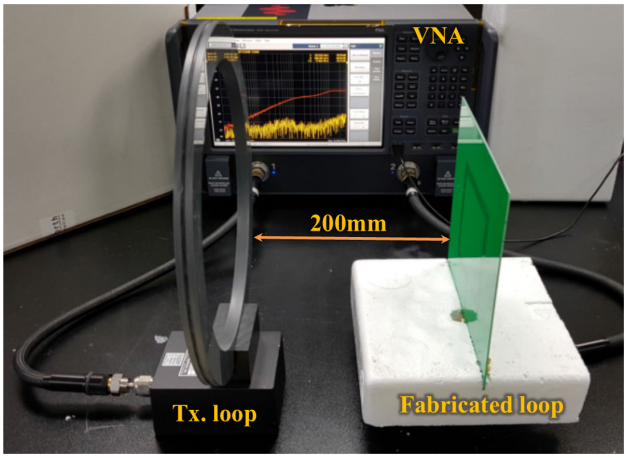

(a)

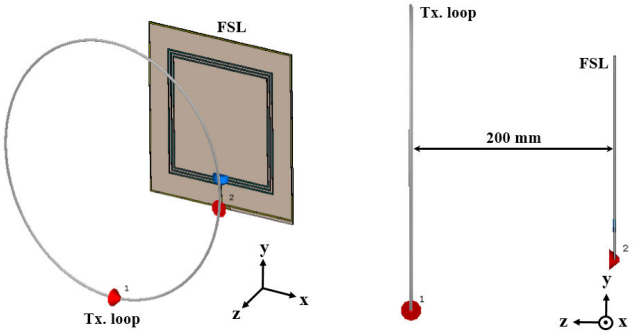

(b)

FIGURE 7. AF of the proposed antenna measurement and simulation environment. (a) Measurement. (b) Simulation.

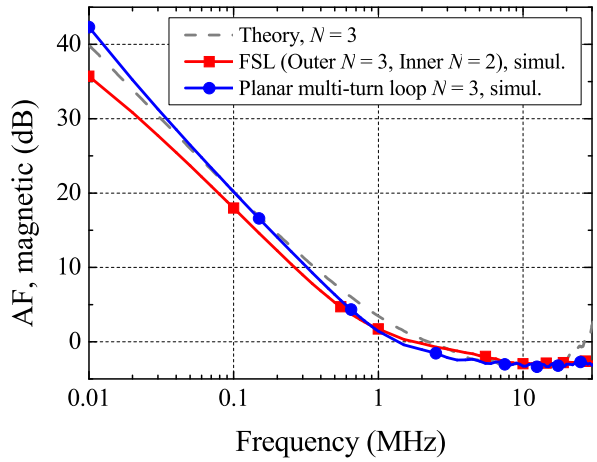

FIGURE 8. AF comparisons of the theoretical results, the FSL (Outer $N = 3$, Inner $N = 2$), and the planar multi-turn loop ($N = 3$).

and planar multi-turn loop (2,547 mm), respectively. It is shown that the AF of FSL in the lower frequency band (10 kHz – 1 MHz) is more improved than the AF of the 3-turns planar loop (Max 6.6 dB @ 10 kHz, Min 0.1 dB @ 1 MHz).

In upper frequency band, the AF level of FSL with the low-pass filter is similar to the multi-turn loop. Therefore, the antenna can be freely designed to meet the target

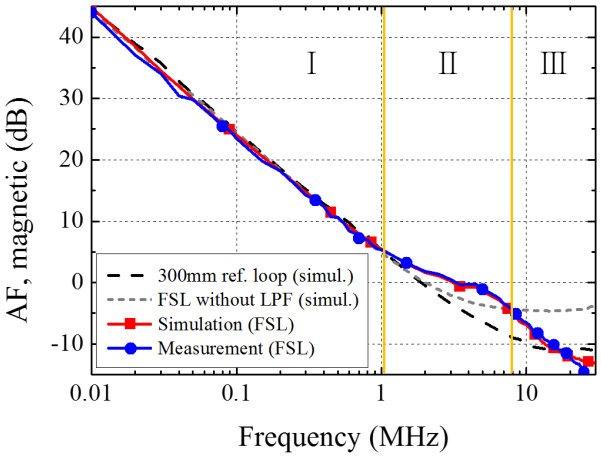

FIGURE 9. AF of the fabricated antenna (220 mm × 220 mm).

AF level by adjusting the number of outer and inner loop turns.

The goal of this paper is to miniaturize a one-turn 300 mm loop antenna and improve the antenna performance at more than 10 MHz. Thus the proposed antenna is optimized to the outer 1-turn and inner 2-turns loop configuration. Fig. 9 shows a comparison of the simulated and measured AF. A good agreement is observed between the simulation and measurement. To verify the characteristic of the proposed antenna, the measured AF is compared with the 300 mm reference loop [3] and the AF of the proposed loop without the low-pass filter. The AF of the fabricated antenna is divided into three regions.

Region 'I' shows the same AF level as the 300 mm reference loop's level although the size is reduced to 220 mm × 220 mm because the outer and inner loops are connected. Region 'II' is the transient region. The AF level rises up to 5.5 dB above the 300 mm reference loop's level due to the skirt characteristic of the 1st-order low-pass filter. Increasing the order of the low-pass filter reduces the AF level in the transient region, but due to the influence of the reactance used in the low-pass filter, the Q value of the loop increases in this region. Thus, this results in very high AF levels at certain frequency. In Region 'III', only the outer lop operates and the AF level is lower than reference loop antenna. Without the low-pass filter, the inductance of the line increases rapidly at more than 10 MHz as shown in Fig. 10.

AFs with different capacitance of low-pass filter and resistance of attenuation resistor are simulated and shown in Fig. 11 and Fig. 12, respectively. Fig. 11 shows that resonant frequency decreases as the C value of the low-pass filter increases. In Fig. 12, there is no current flowing to the inner loop at low R value, so the AF level increases in entire band. In contrast, if the R value is significantly greater than the inner loop, the AF level increases at specific frequency. Based on the above analysis, we have a clear method for controlling the resonant frequency and attenuating the undesired coupled current.

TABLE 2. The loop antenna for SE measurement property comparisons.

	Ref. [3]	Ref. [13]	Ref. [26]	Ref. [27]	Proposed FSL
Operating Frequency	9 kHz – 30 MHz	9 kHz – 400 MHz	10 kHz – 30 MHz	10 kHz – 30 MHz	10 kHz – 30 MHz
Dimension (mm^3)	300 × 300 × 1	50 × 50 × 10	114 × 114 × 40	100 × 100 × 21	220 × 220 × 1.6
Loop structure	1-turn loop	Shielded loop	Multi-turn (ferrite core)	Multi-turn (ferrite core)	Planar multi-turn
AF (dB) @ 10 kHz	45	53.5	34	40.5	43.6
AF (dB) @ 10MHz	-10	23.6	7	-3	-8

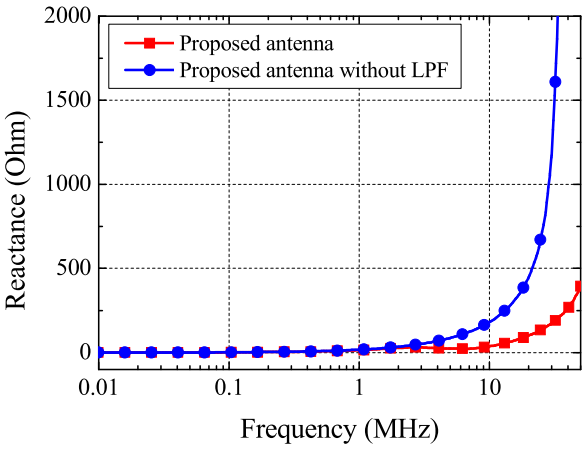

FIGURE 10. Reactance comparisons of the proposed antenna with and without the low-pass filter.

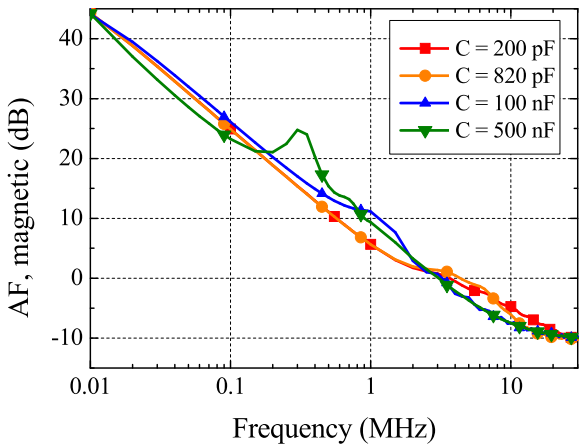

FIGURE 11. Simulated AFs of the proposed antenna by changing of C.

Table 2 compares the operating frequency bands, dimensions, the structure types, and AF levels between the four reference loops and proposed FSL. Although the size of proposed antenna has been reduced to 220 mm × 220 mm, it has equivalent performance to the commercial 300 mm × 300 mm loop. In addition, the planar structure printed on the substrate has advantages that are easier to fabricate than the shielded loop and multi-turn structures.

Fig. 13 shows the current distribution of the proposed antenna at the selected frequencies (10 kHz, 5 MHz, 20 MHz). In Fig. 13(a), the outer loop and the inner loop are connected so that the current direction is the same. Fig. 13(b)

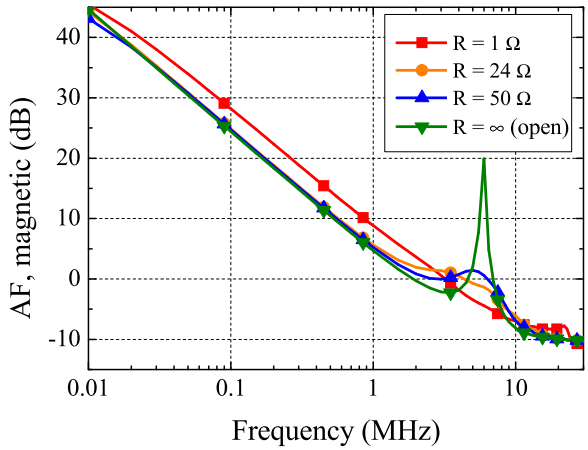

FIGURE 12. Simulated AFs of the proposed antenna by changing of R.

shows the current distribution at 5 MHz, the transition region, indicating that some current also flows through the inner loop. In Fig. 13(c), the current exists in the outer loop, while coupled current flows in the opposite direction on the inner loop with small level. This implies that the coupled current is attenuated sufficiently.

IV. SE MEASUREMENT

SE measurement have been performed to ensure that the proposed FSL is suitable for SE measurement of the small shielding enclosure (size: 600 mm × 600 mm × 650 mm). The SE measurement was followed by the IEEE standard 299.1 [1] in the 10 kHz to 20 MHz bands.

SE measurement setup is shown in Fig. 14. The transmitting loop (A.H.Systems, SAS-564) is connected to a signal generator (KEYSIGHT, N5171B, 9 kHz – 1 GHz) and power amplifier (AR, 10WD1000, 10 W). The receiving loop (proposed FSL) is connected to the spectrum analyzer (KEYSIGHT, N9918A) and the preamplifier (A.H. systems, PAM-5K300).

The distance between the transmitting and receiving loop is 0.6 m, with the door of the small shielding enclosure at the center of the two loops.

The SE of the small shielding enclosure from experiment setup, as written in (6), is calculated [1].

$$\mathrm{SE} = 20\log_{10}\left|\frac{V_1}{V_2}\right| \tag{6}$$

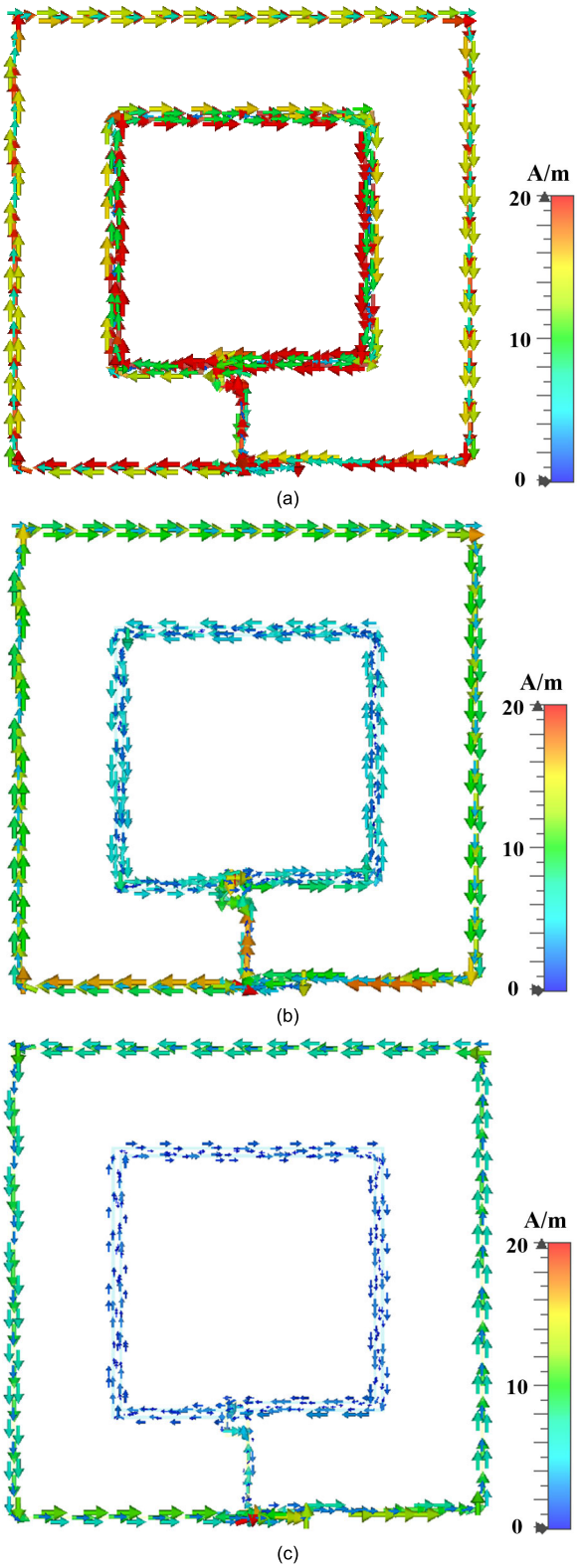

FIGURE 13. Simulated current distribution of the proposed antenna. (a) 10 kHz. (b) 5 MHz. (c) 20 MHz.

where V_1 and V_2 are receiving voltages of FSL in free space and in the shielding enclosure, respectively. Fig. 15 shows the SE measurements of vertical and horizontal polarization

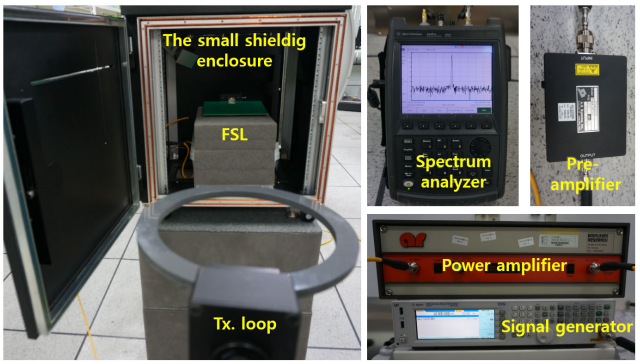

FIGURE 14. The experiment setup of SE using proposed FSL.

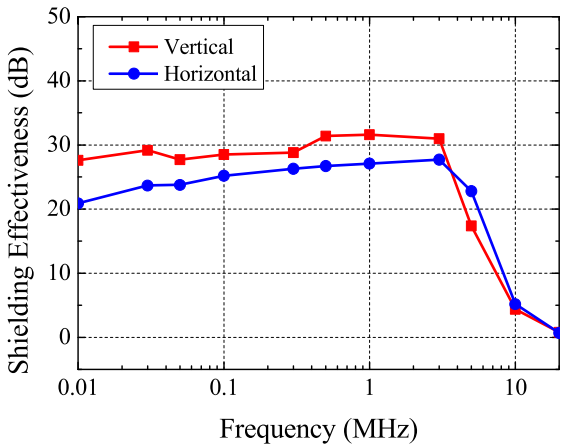

FIGURE 15. The measured SE of small shielding enclosure.

at selected frequencies in the 10 kHz to 20 MHz band. The measured SE average level are 21.1 dB and 19.4 dB in the vertical and horizontal polarizations, respectively.

V. CONCLUSION

An electrically small and frequency selective loop antenna for shielding effectiveness (SE) measurement in low frequency (10 kHz – 30 MHz) band is proposed in this paper. The low-pass filter is placed between outer and inner loops to improve the antenna factor (AF) of the upper frequency band as the number of loop turns increases. The size of the designed antenna is 220 mm × 220 mm, which achieves 46 % reduction of antenna area compared to the conventional 300 mm loop antennas and the antenna preserves the better AF characteristics. From the above results, we conclude that the proposed antenna is suitable for SE measurements of small enclosures.

REFERENCES

[1] *IEEE Standard Method for Measuring the Shielding Effectiveness of Enclosures and Boxes Having All Dimensions Between 0.1 m and 2 m*, Standard 299.1, 2013.
[2] *High Altitude Electromagnetic Pulse (HEMP) Protection for Ground Based Communication Facilities Performing Critical, Time-Urgent Missions: Part 2: Transportable and Mobile Systems*, Standard 59-188, 2017.
[3] SAS-564. *A. H. Systems*. [Online]. Available: http://www.ahsystems.com

[4] R. Araneo and S. Celozzi, "A new EMC antenna for the low-frequency SE measurement of small enclosures," in *Proc. IEEE ISEMC, Int. Symp. EMC, Washington, DC, USA, 2000*, vol. 2, pp. 755–760.
[5] J. E. Lindsay and K. Munter, "Distributed parameter analysis of shielded loops used for wide-band H-field measurements," *IEEE Trans. Instrum. Meas.*, vol. 32, no. 1, pp. 241–244, Mar. 1983.
[6] P. H. Duncan, "Analysis of the moebius loop magnetic field sensor," *IEEE Trans. Electromagn. Compat.*, vol. EMC-16, no. 2, pp. 83–86, May 1974.
[7] O. Aluf, "Moebius loop antenna system stability analysis under parameters variation," in *Proc. IEEE Int. Conf. Microw., Antennas, Commun. Electron. Syst. (COMCAS)*, Nov. 2017, pp. 1–5.
[8] A. Boswell, A. J. Tyler, and A. White, "Performance of a small loop antenna in the 3-10 MHz band," *IEEE Antennas Propag. Mag.*, vol. 47, no. 2, pp. 51–56, Apr. 2005.
[9] E. Suzuki, S. Arakawa, H. Ota, K. I. Arai, and R. Sato, "Optical magnetic field probe with a loop antenna element doubly loaded with electrooptic crystals," *IEEE Trans. Electromagn. Compat.*, vol. 46, no. 4, pp. 641–647, Nov. 2004.
[10] L. L. Libby, "Special aspects of balanced shielded loops," *Proc. IRE*, vol. 34, no. 9, pp. 641–646, Sep. 1946.
[11] J. Dyson, "Measurement of near fields of antennas and scatterers," *IEEE Trans. Antennas Propag.*, vol. 21, no. 4, pp. 446–460, Jul. 1973.
[12] M. Ishii and K. Komiyama, "Impedance method for a shielded standard loop antenna," *IEEE Trans. Instrum. Meas.*, vol. 56, no. 2, pp. 422–425, Apr. 2007.
[13] HFRAE 5163. *Schwarzbeck*. [Online]. Available: http://www.schwarzbeck.de
[14] A. Frikha, M. Bensetti, F. Duval, N. Benjelloun, F. Lafon, and L. Pichon, "A new methodology to predict the magnetic shielding effectiveness of enclosures at low frequency in the near field," *IEEE Trans. Magn.*, vol. 51, no. 3, Mar. 2015, Art. no. 8000404.
[15] T. Hayashi, K. Komiyama, T. Morioka, T. Yamaguchi, and Y. Amemiya, "Measurements of near-field shielding effectiveness by small loop antennas," in *Proc. Conf. Precis. Electromagn. Meas.*, May 2000, pp. 529–530.
[16] T. Mori, K. Shinozaki, and Y. Kaneko, "Improving shielding effectiveness measurements with a spherical dipole antenna," in *Proc. IEEE Symp. Electromagn. Compat.*, Chicago, IL, USA, Aug. 1994, pp. 1–4.
[17] M. Ishii and Y. Yamazaki, "A study on measurement method of shielding effectiveness using loop antenna in low frequency," in *Proc. IEEE Symp. Electromagn. Compat.*, Tokyo, Japan, May 2014, pp. 749–752.
[18] G. Smith, "Radiation efficiency of electrically small multiturn loop antennas," *IEEE Trans. Antennas Propag.*, vol. AP-20, no. 5, pp. 656–657, Sep. 1972.
[19] H. H. Park, C. H. Hyoung, and J. H. Kwon, "Improvement of low-frequency magnetic shielding measurement using rhombic and long rectangular loop antennas," *IEEE Trans. Electromagn. Compat.*, vol. 62, no. 4, pp. 1364–1368, Aug. 2020, doi: 10.1109/TEMC.2019.2942523.
[20] Z. Yan, J. Wang, W. Zhang, Y. Wang, and J. Fan, "A simple miniature ultra-wideband magnetic field probe design for magnetic near-field measurements," *IEEE Trans. Antennas Propag.*, vol. 64, no. 12, pp. 5459–5465, Dec. 2016.
[21] Y. G. Xia, J. Luo, and H. Ye, "A standard shielded loop antenna with load resistor," in *Proc. IEEE 3rd Int. Symp. Microw. Antennas, Propag.*, Oct. 2009, pp. 405–407.
[22] Y. T. Chou and H. C. Lu, "Electric field coupling suppression using via fences for magnetic near-field shielded-loop coil probes in low temperature cofired ceramic," in *Proc. IEEE Int. Symp. Electromagn. Compat.*, Aug. 2011, pp. 6–10.
[23] Y. Arellano, A. Hunt, and O. C. L. Haas, "Evaluation of near-field electromagnetic shielding effectiveness at low frequencies," *IEEE Sensors J.*, vol. 19, no. 1, pp. 121–128, Jan. 2019.
[24] S. R. Best, "Optimizing the receiving properties of electrically small HF antennas," *URSI Radio Sci. Bullet.*, vol. 2016, no. 359, pp. 13–29, Dec. 2016.
[25] E. Kang, T. H. Lim, D. H. Lee, K. B. Kim, S. K. Ryu, and H. Choo, "Design of a small loop antenna operating in VLF band for shielding effectiveness measurement," in *Proc. Int. symp. Antennas Propag.*, Xi'an, China, 2019, pp. 1–2.
[26] E. Kang, T. H. Lim, S. Youn, D. H. Lee, K. B. Kim, and H. Choo, "Design of a miniaturized printed multi-turn loop antenna for shielding effectiveness measurement," *IEEE Access*, vol. 8, pp. 54872–54878, 2020.
[27] S. Youn, T. H. Lim, E. Kang, D. H. Lee, L. B. , and H. Choo, "Design of a miniaturized rectangular multiturn loop antenna for shielding effectiveness measurement," *Sensors.*, vol. 20, no. 11, pp. 1–10, Jun. 2020.
[28] C. A. Balanis, *Antenna Theory: Analysis and Design*, 4th ed. New York, NY, USA: Wiley, 2005, pp. 235–277.
[29] (2019). *CST Microwave Studio, Dassault Systems*. [Online]. Available: http://www.3ds.com
[30] M. Ishii and K. Komiyama, "Estimation of uncertainty of calibration for loop antennas by three-antenna method using automatic network analyzer," in *Proc. 67th ARFTG Conf.*, San Francisco, CA, USA, Jun. 2006, pp. 156–163.

KI BAEK KIM received the B.S., M.S., and Ph.D. degrees in radio science and engineering from Chungnam National University, Daejeon, South Korea, in 2010, 2012, and 2021, respectively. Since 2012, he has been a Senior Researcher with the affiliated research organization of the Electronics and Telecommunications Research Institute (ETRI), Daejeon. His research interests include electrically small antennas for shielding effectiveness (SE), antenna array for radar systems, and EMI/EMC studies.

DAE HEON LEE received the B.S., M.S., and Ph.D. degrees in electronics and radio engineering from Kyungpook National University, Daegu, South Korea, in 1999, 2001, and 2013, respectively. Since 2003, he has been a Senior Researcher with the affiliated research organization of the Electronics and Telecommunications Research Institute (ETRI), Daejeon. His research interests include UWB antennas, slot antenna with band-notched function, GPS applications, active antenna arrays, and shielding effectiveness (SE) measurement.

SEUNG KAB RYU received the B.S. degree in aviation electronics from Korea Aviation University, South Korea, in 1999, the M.S. and Ph.D. degrees from the School of Mechatronics, Gwangju Institute of Science and Technology (GIST), Gwangju, South Korea, in 2001 and 2014, respectively. From 2001 to 2004, he was with Millitron Inc., as a Senior Engineering Staff for the development of the millimeter-wave transceiver and the satellite outdoor unit. He is currently with the Infrastructure Protection Research and Development Department, Electronics and Telecommunications Research Institute (ETRI), Daejeon, South Korea. His research interests include high power plasma physics, high voltage fast transient pulse measurement with RF technology, high voltage sub-nanosecond pulsed power source, and HPEM protection device for antenna line, such as plasma limiter, intentional electromagnetic interference (IEMI) immunity research on microwave, and wireless equipment.

HOSUNG CHOO (Senior Member, IEEE) received the B.S. degree in radio science and engineering from Hanyang University, Seoul, South Korea, in 1998, and the M.S. and Ph.D. degrees in electrical and computer engineering from The University of Texas at Austin, in 2000 and 2003, respectively. In September 2003, he joined the School of Electronic and Electrical Engineering, Hongik University, Seoul, where he is currently a Professor. His research interests include electrically small antennas for wireless communications, reader and tag antennas for RFID, on-glass and conformal antennas for vehicles and aircraft, and array antennas for GPS applications.